mathematics

MDPI

Article

Capsule Endoscopy Image Enhancement for Small Intestinal Villi Clarity

Shaojie Zhang [1], Yinghui Wang [1,2,*], Peixuan Liu [1,*], Yukai Wang [1], Liangyi Huang [3], Mingfeng Wang [4] and Ibragim Atadjanov [5]

[1] School of Artificial Intelligence and Computer Science, Jiangnan University, Wuxi 214122, China; 7213107006@stu.jiangnan.edu.cn (S.Z.); ericwangyk22@163.com (Y.W.)
[2] Engineering Research Center of Intelligent Technology for Healthcare, Ministry of Education, Wuxi 214122, China
[3] School of Computing and Augmented Intelligence, Arizona State University, Tempe, AZ 85281, USA; lhuan139@asu.edu
[4] Department of Mechanical and Aerospace Engineering, Brunel University London, London UB8 3PH, UK; mingfeng.wang@brunel.ac.uk
[5] Department of Computer Engineering, Tashkent University of Information Technologies Named after Muhammad al-Khwarizmi, Tashkent 100084, Uzbekistan; ibragim.atadjanov@gmail.com
* Correspondence: wangyh@jiangnan.edu.cn (Y.W.); liupeixuan2019@163.com (P.L.)

Abstract: Wireless capsule endoscopy (WCE) has become an important tool for gastrointestinal examination due to its non-invasive nature and minimal patient discomfort. However, the quality of WCE images is often limited by built-in lighting and the complex gastrointestinal environment, particularly in the region filled with small intestinal villi. Additionally, the morphology of these villi usually serves as a crucial indicator for related diseases. To address this, we propose a novel method to enhance the clarity of small intestinal villi in WCE images. Our method uses a guided filter to separate the low- and high-frequency components of WCE images. Illumination gain factors are calculated from the low-frequency components, while gradient gain factors are derived from Laplacian convolutions on different regions. These factors enhance the high-frequency components, combined with the original image. This approach improves edge detail while suppressing noise and avoiding edge overshoot, providing clearer images for diagnosis. Experimental results show that our proposed method achieved a 45.47% increase in PSNR compared to classical enhancement algorithms, a 12.63% improvement in IRMLE relative to the original images, and a 31.84% reduction in NIQE with respect to the original images.

Keywords: gain factor; images; small intestinal villi; wireless capsule endoscopy

MSC: 68U10; 92C55

Citation: Zhang, S.; Wang, Y.; Liu, P.; Wang, Y.; Huang, L.; Wang, M.; Atadjanov, I. Capsule Endoscopy Image Enhancement for Small Intestinal Villi Clarity. *Mathematics* **2024**, *12*, 3317. https://doi.org/10.3390/math12213317

Academic Editor: Konstantin Kozlov

Received: 22 September 2024
Revised: 14 October 2024
Accepted: 14 October 2024
Published: 23 October 2024

1. Introduction

Wireless capsule endoscopy (WCE) offers an effective means of observing the internal structures of the gastrointestinal tract while effectively alleviating patient discomfort [1,2]. However, owing to the limited illumination power of WCE and the complexity of the gastrointestinal environment, the images captured by WCE are often unclear, particularly in the small intestine where abundant tiny villi exist. The magnified section of the true structure of the human small intestine, as shown in Figure 1 [3], reveals the surface covered with tiny villi responsible for absorbing nutrients. In contrast, Figure 2 depicts an actual image of the small intestine captured by WCE. It is evident that the images captured by WCE do not adequately demonstrate the structure of small intestine villi, which is a common issue in such images. However, the morphology of small intestine villi serves as an important basis for diagnosing conditions such as indigestion and malabsorption. When

lesions occur, the morphology of the villi may change, possibly manifesting as shortening, thickening, or even complete loss of the original structure. Therefore, enhancing techniques to highlight the microstructure and edge details of villi can assist physicians in better observing and diagnosing small intestine lesions, identifying the location and severity of lesions more accurately, and thus providing more personalized and accurate treatment plans for patients [4,5]. To the best of our knowledge, there are no articles in the literature reporting methods for enhancing WCE images to render the villi more clearly visible.

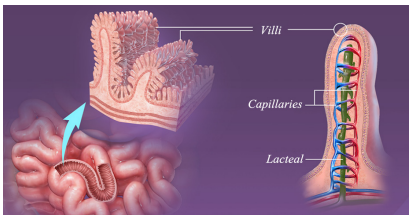

Figure 1. Diagram of human small intestine structure.

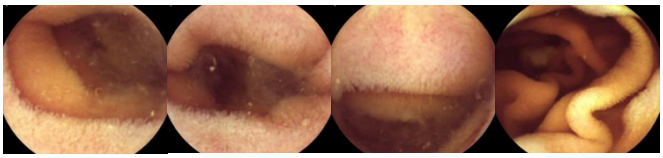

Figure 2. WCE images of the small intestine with villi.

So far, there have been numerous related methods for enhancing small intestine images. The commonly used classic methods can be classified into three categories: Histogram Equalization (HE) methods [6–10], Retinex-based methods [11–18], and Unsharping mask (USM) methods [19–25], etc. Among them, the USM [20] methods are the most advantageous approach in emphasizing image detail information. Methods based on HE enhance images by remapping the input image's gray levels using the probability distribution of grayscale levels. Nonetheless, these methods encounter problems like inadequate enhancement, excessive enhancement, and notable noise amplification in the resulting enhancements. The Retinex-based methods view an image as a combination of light and reflection components, enhancing the image by adjusting the corresponding components. However, the effect of highlighting image detail information using the Retinex-based methods is not very ideal. Specifically, traditional USM methods use a fixed gain factor to enhance high-frequency components. Subsequently, some scholars improved the USM methods by proposing adaptive gain factors based on local image information [25]. Clearly, the aforementioned methods were not specifically designed for enhancing small intestinal villi. Moreover, our experiments have revealed [26] that they also do not achieve the desired effect of highlighting small intestinal villi. In addition, in the past decade, many scholars have proposed methods for endoscope image enhancement based on USM [19,22,23]. While USM methods have the potential to emphasize image details, these methods have not adequately considered the balance between detail enhancement and noise suppression. This imbalance results in issues such as edge overshooting and amplified noise in the enhanced results. Therefore, they are not directly suitable for enhancing small intestine villi in WCE images.

To address the above issue, this paper proposes an image enhancement method aimed at enhancing the clarity of small intestinal villi. The method is based on two key functions: the light gain function and the gradient gain function. The light gain function combines light information to enhance high-frequency components while suppressing noise in darker areas. This is crucial because it helps to improve the visibility of details in regions that are typically poorly illuminated in WCE images. On the other hand, the gradient gain function enhances the high-frequency components of capsule endoscopy small intestine villi images based on gradient information. This dual-function approach not only enhances

the fine details of small intestine villi but also mitigates the occurrence of edge overshoot phenomena. The main innovations in this paper can be summarized as follows:

- We have proposed a gain factor construction method, which relies on the light gain function and gradient gain function we construct. The light gain function combines light information to enhance high-frequency components while suppressing noise in darker areas. The gradient gain function enhances the high-frequency components of capsule endoscopy the small intestine villi images based on gradient information. This enhances the fine details of small intestine villi while concurrently mitigating the occurrence of edge overshoot phenomena.
- We have developed a method for enhancing the clarity of tiny villi on the surface of the small intestine based on the WCE image. This method not only provides clearer and more detailed images, offering medical workers or internal autonomous robots more opportunities for precise localization of lesions, but also greatly enhances their understanding and assessment capabilities of the condition, providing strong support for accurate diagnosis and treatment.

2. Related Work

Three common types of image enhancement methods include HE methods [6–10], Retinex-based methods [11–18], and USM methods [19–25].

The HE methods [6] partition the image histogram by identifying local minima and assigning specific grayscale ranges to each partition. Subsequently, these partitions are equalized separately to enhance the image. In [10], the HE methods were improved by introducing brightness constraints to achieve image detail enhancement while preserving brightness. However, methods based on HE typically lead to insufficient or excessive enhancement of fine details, making them unsuitable for highlighting the villi in small intestine images.

The Retinex method views a scene in the human eye as a product of reflection and illumination components [17], enhancing the scene image by adjusting these components accordingly [11]. In [18], the decomposed reflection component was directly regarded as the enhancement result, but it could lead to the occurrence of halos and a loss of naturalness. Afterward, scholars proposed a variational model [15] for estimating reflection and illumination components, adjusting and combining these components to reconstruct the enhanced effect. The Retinex-based methods' effectiveness on the fine details of microscopic villi structures is limited.

The USM methods primarily enhance image details and edge information by emphasizing the image's high-frequency content. In [24], the Laplacian operator was utilized for image filtering to enhance the image, but this method has many parameters and involves heavy computation. In [25], the difference between the iterative median filtering and the original image was used to obtain the details of the image. However, this approach resulted in halo artifacts along the edges, with limited enhancement in smoothly lit areas. In [19], a Gaussian filter was applied to WCE images to accentuate image details, but this process could lead to issues like overshooting and excessive noise amplification. In [20], a hybrid median filter [27] calculated the median values for square, cross-shaped, and diagonal windows to replace the central pixel of the filtering window. However, the literature did not take into account the impact of noise during image enhancement. In [21], the high-frequency components of a guided image were added to the low-frequency components of the original image under the control of a gain factor. This factor was obtained using an optimization function based on guided filtering [28] and weighted guided filtering [29]. Additionally, in [21], the authors introduced a convolutional neural network to derive the gain factor. However, due to the considerable difficulty in obtaining in vivo data, this method is not applicable to images in an in-body environment. Although these methods improve upon USM techniques by enhancing filters and gain factors to boost detail enhancement, they still suffer from issues like edge overshooting and noise amplification when applied to image enhancement. The main problem lies in how gain factors are configured.

To address this, we employed guided filtering [28] to filter WCE small intestine villi images, obtaining low-frequency components with well-preserved edges and gradients. We constructed light gain functions based on the low-frequency components of different regions in small intestine villi images to adaptively generate light gain factors. Furthermore, we created adaptive gradient gain factors by building gradient gain functions using the Laplacian operator's convolution results in various areas of small intestine villi images. Ultimately, we combined the previously mentioned light and gradient gain factor to create the adaptive gain coefficients needed for enhancing the USM method, thereby improving the USM approach. Our method effectively enhances the clarity of small intestine villi details while suppressing noise in darker regions and preventing edge overshooting.

3. Math

The image enhancement method framework for small intestine villi clarity in WCE is illustrated in Figure 3.

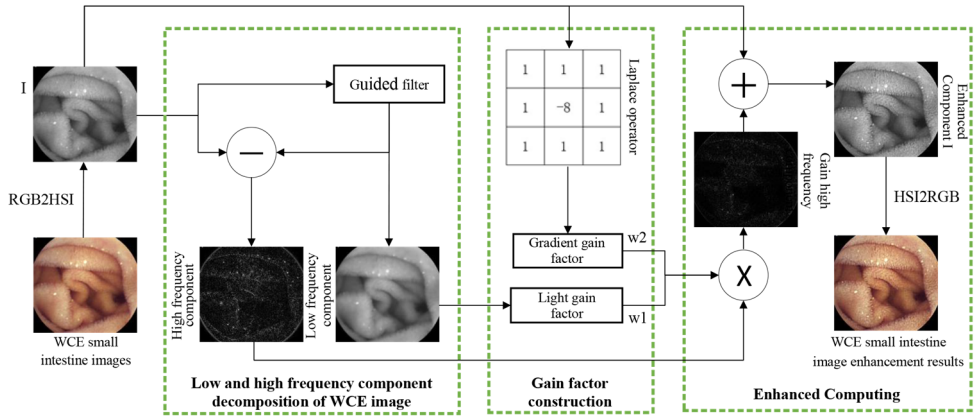

Figure 3. Methodological framework.

Firstly, the small intestine image was filtered and smoothed through the edge-preserving and gradient-preserving properties of the guided filter to obtain its low-frequency component. Then, the high-frequency component was obtained by subtracting the filtered low-frequency component from the original image.

Secondly, a light gain function was constructed based on the low-frequency components of different regions of the WCE image to adaptively generate the light gain factor w1, which enhanced the high-frequency component while suppressing the noise in the dark regions. In addition, based on the Laplacian operator of different regions of the WCE small intestine image, a gradient gain function was obtained by convolution to adaptively generate the gradient gain factor w2. A larger w2 value was obtained where the convolution result value was smaller to highlight the edge details, and conversely, a smaller w2 value was taken to prevent the occurrence of edge overshoot problems.

Finally, we multiplied the obtained light gain factor, gradient gain factor, and high-frequency component in a matrix to obtain the gain high-frequency component and then superimposes the gain high-frequency component on the original image, achieving the purpose of enhancing the small intestine image and supporting the adaptability of the method.

3.1. Low-High Frequency Component Decomposition

The USM is a sharpening enhancement technology, and the calculation formula as shown in (1).

$$ZI(x,y) = I(x,y) + k(I(x,y) - \overline{I}(x,y)) \quad (1)$$

where $ZI(x, y)$ is the enhanced image, I denotes the original image, and k stands for the gain coefficient, which controls the degree of enhancement. A higher value of k results in a

more pronounced sharpening effect. $\overline{I}(x, y)$ represents the image after low-pass filtering, which is the low-frequency component.

As can be seen, the essence of USM was to obtain the high-frequency component by subtracting the low-frequency component from the original image. Then, the high-frequency component was amplified by multiplying it with the gain coefficient k. Finally, the amplified high-frequency component was superimposed on the original image to obtain the enhanced image $ZI(x, y)$, achieving the purpose of enhancing the edges of the image. In order to obtain a more accurate high-frequency component, it is crucial to select a suitable low-pass filter to obtain a low-frequency component with good edge preservation. This can enhance high-frequency details in a targeted manner without over-amplifying noise.

The guided filtering [28] exhibited a linear relationship between the guided image and the output image as shown in (2).

$$q_i = a_m G_i + b_m, \forall i \in \omega_m \tag{2}$$

where G represents the guided image, q denotes the output image, i and m are pixel indices, ω_m stands for the square window located at position, a_m and b_m are the coefficients of the linear function at position m.

The coefficients a_m and b_m in (2) were obtained by minimizing the linear cost function, as shown in (3).

$$\mathrm{E}(a_m, b_m) = \sum_{i \in \omega_m} \left[(a_m G_i + b_m - p_i)^2 + \varepsilon {a_m}^2 \right] \tag{3}$$

where p represents the input image, and ε is a regularization parameter used to prevent a_m from becoming too large.

Taking the gradient on both sides of (2) simultaneously revealed that the guided image had a similar gradient to the output image. This indicates that the guided filter exhibited good edge-preserving characteristics. The guided filter achieved excellent edge preservation by leveraging the linear relationship between the guidance image and the output image. Therefore, this paper initially converted the WCE small intestine image from the RGB color space to the HSI color space. Subsequently, a guided filter was employed to smooth and filter the I component of the small intestine image in the HSI color space, thereby obtaining its low-frequency component.

3.2. Gain Factor Construction

This section encompasses two aspects: the construction of light gain factor and the construction of gradient gain factor.

3.2.1. Light Gain Factor Construction

Due to the complex in-body environment and limited illumination of the WCE, WCE images exhibit areas that are either too dark or too bright, with dark regions being particularly noisy, as shown in Figure 2. Traditional USM methods do not account for the impact of light, resulting in post-enhancement images with noisy dark regions and insufficient detail enhancement in other areas. To address this, this paper incorporated light gain factors as part of the enhancement coefficient k in (1). The light gain factors in different regions of WCE images were obtained through a light gain function, as depicted in (4).

$$\mathrm{w1} = \begin{cases} 0.5 \sin(\overline{I}(x, y) \cdot \pi), \overline{I}(x, y) < Mean \\ \sin(\overline{I}(x, y) \cdot \pi), otherwise \end{cases} \tag{4}$$

where (x, y) are the pixel coordinates of the image, and $\overline{I}(x, y)$ is the mean.

Since the light changes slowly and smoothly to low-frequency information, the low-frequency information $\overline{I}(x, y)$ obtained by the guided filter was used as the light information of the WCE image in this paper. The light gain function is shown in Figure 4. When the brightness of WCE image was less than the mean, it indicated the dark areas of the WCE image. The method described in this paper acquired the light gain factor using a

compressed sine function. Subsequently, this light gain factor was incorporated into the gain coefficient of (1). This process enhanced high-frequency information in dark areas while simultaneously suppressing noise in those regions. When the brightness of the WCE image surpassed the mean, a sine function was utilized to derive the light gain factor. From Figure 4, we can observe that the light gain factor was notably higher for moderate brightness in WCE images compared to bright areas. As brightness increased, the light gain factor decreased. Leveraging this pattern, the derived light gain factor could effectively enhance high-frequency information in WCE images with moderate brightness. As a result, post-enhanced WCE images exhibited richer details, and this approach effectively achieved adaptive control of the light gain factor.

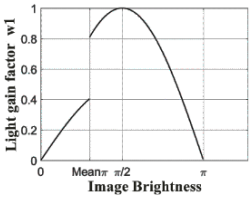

Figure 4. The light gain function reflects the variation law of light gain factor with light intensity.

3.2.2. Gradient Gain Factor Construction

Traditional USM methods enhance image details using a fixed gain coefficient across different edges. Although these methods enhance the image details, the lack of appropriate gain coefficients at the edges leads to edge overshooting. If a greater gain factor is applied to accentuate the details of small intestine villi images while simultaneously utilizing a smaller gain factor at the image edges, edge overshooting is effectively prevented. It is evident that this adaptive implementation of WCE small intestine image enhancement is very necessary. To this end, this paper calculates gradient gain factors for specific regions using the gradient gain function. These factors were subsequently integrated into the gain coefficient of (1) to achieve adaptive enhancement of WCE small bowel images. The gradient gain function w2 is shown in (5).

$$\mathrm{w2}(x,y) = \begin{cases} e^{\frac{\ln 1.5}{0.1}\cdot\nabla I} - 0.5, \ \nabla I < 0.1 \\ e^{3(-\nabla I + 0.1)}, \ otherwise \end{cases} \tag{5}$$

where (x, y) are the image pixel coordinates. ∇I represents the edge information of the image, obtained as the absolute value of the result after convolution and normalization of the original image with the Laplace operator template in Figure 5.

1	1	1
1	−8	1
1	1	1

Figure 5. The Laplacian operator template.

As shown in Figure 5, the Laplacian operator template can highlight the areas with drastic gray-level changes in the image when detecting edges, thus helping to identify important features such as object contours and boundaries in the image. When processing WCE small intestinal villi images, this template can be used to determine the edge information in the image. Then, according to the gradient gain function, the gradient gain factors of different regions can be obtained to achieve adaptive enhancement of the image. In areas with rich image details, due to the large changes in pixel values, a larger gradient gain factor may be obtained after template calculation, thereby enhancing the detailed

information in these areas. In the image edge area, in order to prevent edge overshoot, a smaller gradient gain factor can be obtained to make the edge more natural.

Figure 6 depicts the gradient gain function. We observed rapid growth in the gradient gain function when the edge information value of the WCE small intestine villi image was less than 0.1. This allowed the small intestine villi image to quickly obtain a larger gradient gain factor in regions where the edge information value was relatively small. Later, the gradient gain factors were introduced into the gain coefficient to achieve the goal of enriching image detail information. Conversely, when the edge information value of the WCE small intestine villi image exceeded 0.1, the slope of the function curve gradually decreased, resulting in a slow reduction of the gradient gain factor. Even in this scenario, the small intestine villi image still required a relatively large gradient gain factor. When the edge information value approached 1, representing the edges in the image, the gradient gain factor was smaller to prevent edge overshoot.

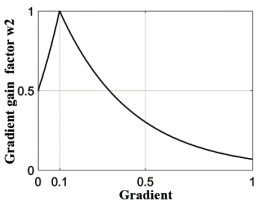

Figure 6. The gradient gain function reflects the variation pattern of the gradient gain factor with the image gradient.

3.3. Enhanced Computing

To highlight the details of WCE small intestine villi images while preventing excessive noise and overshooting, this paper combined the light gain factor and refers to (1), which was obtained by (4) and (5), so as to realize the adaptive enhancement of WCE small bowel image. The adaptive gain coefficient is shown (6).

$$\mathrm{k} = \alpha \cdot w1 \cdot w2 \tag{6}$$

where α is the control maximum parameter, $w1$ is the light gain factor, and $w2$ is the gradient gain factor.

After obtaining the adaptive gain coefficient, we multiplied it with the high-frequency component obtained in Section B to obtain the gain high-frequency component of the WCE small intestine image. Then, we integrated the enhanced component I into the I component of the original input image of the WCE small intestine to strengthen the image's edge. Finally, we converted from the HSI color space to the RGB color space to obtain the clarified WCE small bowel villi image.

4. Experiments and Results Evaluation

4.1. Experimental Data Selection

To the best of our knowledge, there is currently no publicly available standard dataset specifically dedicated to small intestine villi. Therefore, in the absence of a standardized dataset for small intestine images, and to effectively demonstrate the application effectiveness of the method for enhancing small intestine villi clarity in real medical scenarios, this paper selected 50 WCE images from the human small intestine as the dataset for image enhancement. These images were actual small intestine images of patients collected by capsule endoscopy at Jiangnan University Affiliated Hospital, aiming to validate the effectiveness of the proposed method. To protect patient privacy, personal information has been removed from these images. The experiments in this paper were performed on a PC with an eight-core Intel i5-8520U, 1.80 GHz CPU, and 8GB RAM, implemented using MATLAB 2019a.

4.2. Evaluation Metrics

This paper focuses on the enhancement treatment of small intestinal villi, thus concentrating on the preservation of details and the improvement of clarity. Selecting appropriate evaluation criteria allows for accurate quantification of the algorithm's ability to protect image details and enhance clarity, thereby validating the effectiveness of our image enhancement algorithm. Therefore, this paper used the Peak Signal-to-Noise Ratio (PSNR), Intensity Restricted Average Local Entropy (IRMLE), and Natural Image Quality Evaluator (NIQE) for evaluations.

PSNR is widely used to measure image attributes such as texture detail enhancement, detail preservation, and contrast enhancement. A higher PSNR value indicates good image quality after processing, while preserving more edges and texture details. The PSNR expression is shown in (7).

$$PSMR = 10 \times \log_{10} \frac{L^2}{MSE} \tag{7}$$

where L denotes the maximum intensity in the image. The MSE is the mean square error between the reference image and the image to be measured, and its expression is shown in (8).

$$MSE = \frac{1}{MN} \sum_{i=0}^{\mathrm{m}-1} \sum_{j=0}^{n-1} (I(i,j) - K(i,j))^2 \tag{8}$$

where $m \times n$ is the image size. I and K represent the reference image and the pending image, respectively.

In medical imaging, PSNR may have certain limitations. In the context of enhancing small intestinal villi images in this study, if the original WCE images have noise, focusing only on methods to achieve a high PSNR value may enhance the noise while enhancing the desired details. This may lead to inaccurate interpretations by medical professionals because although the PSNR value appears good, the enhanced image may still have poor visual quality. Therefore, we combined multiple evaluation metrics, namely the IRMLE and NIQE metrics mentioned below, to ensure the accuracy of the evaluation.

Compared with natural images, WCE images have limited contrast, and the distribution of their intensities in the whole dynamic range is not uniform. Therefore, the IRMLE proposed in [19] was used to evaluate the richness of detail information of WCE images, and the larger the value was, the better the detail enhancement effect was. The IRMLE expression is shown in (9).

$$IRMLE = \frac{1}{mn} \sum_{i=1}^{m} \sum_{j=2}^{n} LE(i,j) \cdot \textstyle\sum_{r_N=1/3}^{r_N=1} p(r_N) \tag{9}$$

where $p(r_N)$ denotes the probability that the image level is r_N, $LE(i,j)$ is the entropy of a 9×9 window with (i,j) as the pixel center, and the entropy LE is defined as shown in (10).

$$LE = -\sum_{l=r_0}^{r_{L-1}} p(l) \cdot \log_2 p(l) \tag{10}$$

where $p(l)$ represents the probability of the image level being l.

IRMLE is more sensitive to noise in the image, especially in the image's detailed areas. Unlike PSNR, which only focuses on the power ratio of signal to noise, IRMLE measures the image quality from the perspective of detailed information. When the image enhancement method introduces noise while enhancing details, IRMLE can reflect this change through its calculation method, providing more accurate information for evaluating image quality and avoiding the impact of noise on details by simply pursuing a high PSNR value.

The NIQE [30] is the no-reference evaluation image assessment metric, and the smaller its value is, the better the quality is. The NIQE does not rely on the original image or reference image and can directly assess the quality of an image. Small intestine villi images

typically have complex textures and details, and the NIQE considers both local and global characteristics of the image, including contrast, texture clarity, and other aspects. Its quality is expressed as the distance between the NSS feature model and the MVG fitted to the features extracted from the test image, and its expression is shown in (11).

$$D(V_1, V_2, \sum_1, \sum_2) = \sqrt{((V_1 - V_2)^T (\frac{\sum_1 + \sum_2}{2})^{-1} (V_1 - V_2))} \tag{11}$$

where v_1, v_2, $\sum_1$, $\sum_2$, represent the mean vector and covariance of the MVG model for natural and test images, respectively.

The NIQE can analyze the local features and texture information of the image to determine whether noise has a negative impact on image quality. If the noise in the enhanced image increases, resulting in a decrease in texture clarity, the NIQE value will reflect this change, thus compensating for the deficiency of PSNR in this regard.

We evaluated the performance of enhanced small intestinal villi images in subjective clinical aspects through objective indicators. Although there is no one-to-one correspondence between objective indicators and subjective evaluations, there is usually a positive correlation. For example, an image with a higher PSNR value is usually considered to be closer to the original image with less distortion, which is crucial for doctors who need to compare enhanced images with their own prior knowledge and experience. The IRMLE value shows that enhanced detail information can make the visualization effect of small intestinal villi better, which is of great benefit to clinical diagnosis. Similarly, a lower NIQE value means that the image quality has been improved. Through objective indicators, we can strongly prove that our method is of great significance in clinical practice.

4.3. Parameter Variation Experiment

The parameter α is a constant that controls the enhancement intensity at each point while avoiding excessive enhancement. The specific value of needs to be determined through experimentation. Figure 7 illustrates the variation of relevant evaluation parameters when the parameter takes different values in (6). As the value of α increased, we observed an increase in both the level of detail enhancement and noise. This phenomenon indicates that the parameter α is positively correlated with the richness of detail information in WCE small intestine villi images and inversely correlated with the degree of noise. As α increased, the NIQE value initially decreased and then increased. When α was set to 4, the NIQE value reached its minimum at 3.5015, while the PSNR value was 33.1341, and the IRMLE value was 2.5345. Overall, the image quality was at its best, effectively maintaining the original small intestine structure, enhancing the clarity of small intestine villi details, and preventing excessive noise and edge artifacts. In this paper, the value of was selected as 4.

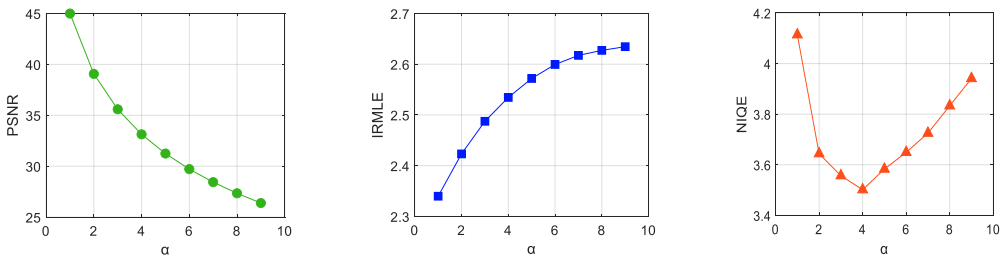

(**a**) PSNR (**b**) IRMLE (**c**) NIQE

Figure 7. The parameter α takes different values, ranging from 1 to 9, to evaluate the enhancement results of WCE small intestine images. (**a**) shows the trend of PSNR changes, (**b**) illustrates the trend of IRMLE changes, and (**c**) demonstrates the trend of NIQE changes.

When the value of α was determined to be 4, the influence of the light gain factor $w1$ and the gradient gain factor $w2$ on the proposed method could be further discussed. w1(x, y) and $w2(x, y)$ are adaptive functions at each pixel point (x, y) on the image, and their values change depending on the pixel point (x, y). Therefore, experiments were conducted on three representative WCE small intestine villi images, as shown in Figure 8a–c, to examine the effects of these factors on enhancing small intestine villi images. Table 1 provides the evaluation metric values for the enhanced results in Figure 8.

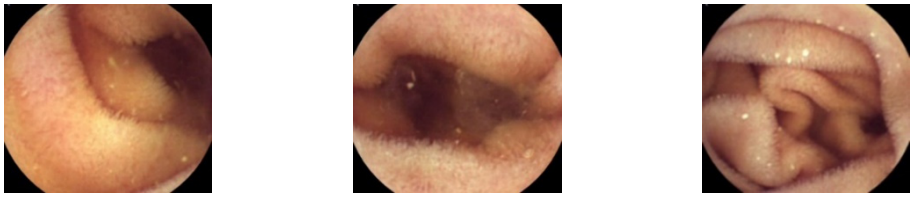

(**a**) original (**b**) original (**c**) original

Figure 8. Parameter w1 and w2 ablation experiments. (**a**–**c**) represent the original WCE small intestine images.

Table 1. Evaluation index values of WCE small intestine enhancement results in ablation experiments.

The Ablation Part		PSNR	IRMLE	NIQE
Light gain factor (w1)	image (a)	29.7378	**2.1777**	3.7072
	image (b)	29.1702	**1.8249**	4.9491
	image (c)	27.7551	**2.7342**	3.7062
Gradient gain factor (w2)	image (a)	32.1409	2.1517	3.6763
	image (b)	31.7118	1.8097	4.9391
	image (c)	30.2093	2.7293	3.6369
w1 + w2	image (a)	**34.2702**	2.0775	**3.6381**
	image (b)	**33.7453**	1.7136	**4.8975**
	image (c)	**32.2204**	2.6868	**3.4683**

When considering only the light gain factor, we observed that it had the best IRMLE value compared to the other two cases, but it exhibited the worst PSNR and NIQE values. This suggests that when only the light gain factor is considered, although the noise in dark areas is suppressed, there is an excessive enhancement of edge details in WCE small intestine villi images. Alternatively, when considering only the gradient gain factor, although the IRMLE value decreased compared to when considering only the light gain factor, the PSNR and NIQE values showed some improvement. However, compared to the case of jointly considering both the light gain factor and the gradient gain factor, the PSNR and NIQE values were still relatively poorer. This suggests that the edge details of WCE small intestine villi images are adaptively enhanced, but there is an excessively enhanced noise in dark areas. When jointly considering both the light gain factor and the gradient gain factor, the PSNR and NIQE values were optimal. This phenomenon indicates effective enhancement of edge details in WCE small intestine villi images while suppressing excessive noise, resulting in the best visual effect.

As shown in Figure 9, the highlighted results of small intestine villi clarification in WCE are presented. The parameters used for enhancement were derived from the experimental results mentioned earlier. In Figure 9e–h, the villi within the blue boxes are notably clearer compared to the original images. The method employed in this paper incorporates adaptive gradient enhancement, resulting in enhanced villi without the occurrence of edge artifacts. In addition, the green boxes in Figure 9e–h represent enhanced dark areas. The original images in Figure 9a–d exhibited limited information and were filled with noise in these dark regions. However, the method introduced in this paper employed light gain factors to suppress noise in dark areas, as evident in the enhanced results. Furthermore, it is

apparent from Figure 9 that the proposed method effectively highlights the small intestine villi, which provides medical professionals with improved image clarity for diagnosing medical conditions. In clinical diagnosis, it can more accurately determine the location and development of diseases.

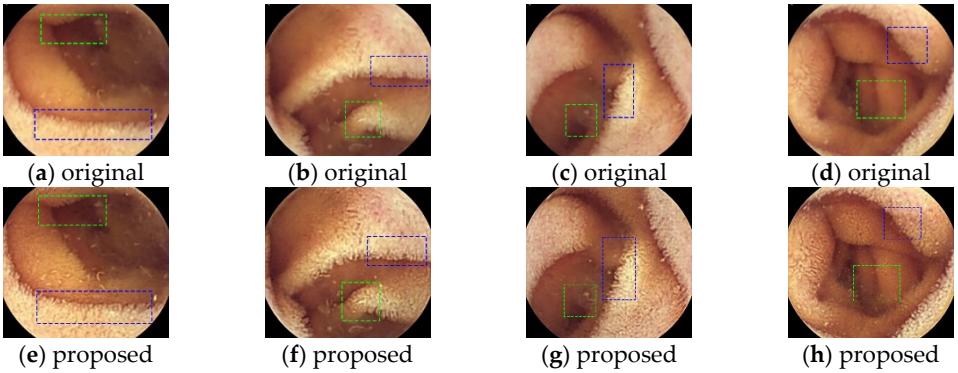

Figure 9. WCE small intestinal villi highlighting results. (**a**–**d**) are the original input images of WCE small intestine, and (**e**–**h**) are the corresponding results after enhancement using the method of this paper, respectively. The blue box was selected for the villi-rich area of the small intestine, and the green box was selected for the dark area of the small intestine.

To facilitate closer examination, Figure 10 depicts selected examples using the small intestine's original input images from Figure 9a,c and the enhanced results with highlighted villi from Figure 9e,g, allowing for a more detailed observation of small intestine villi details.

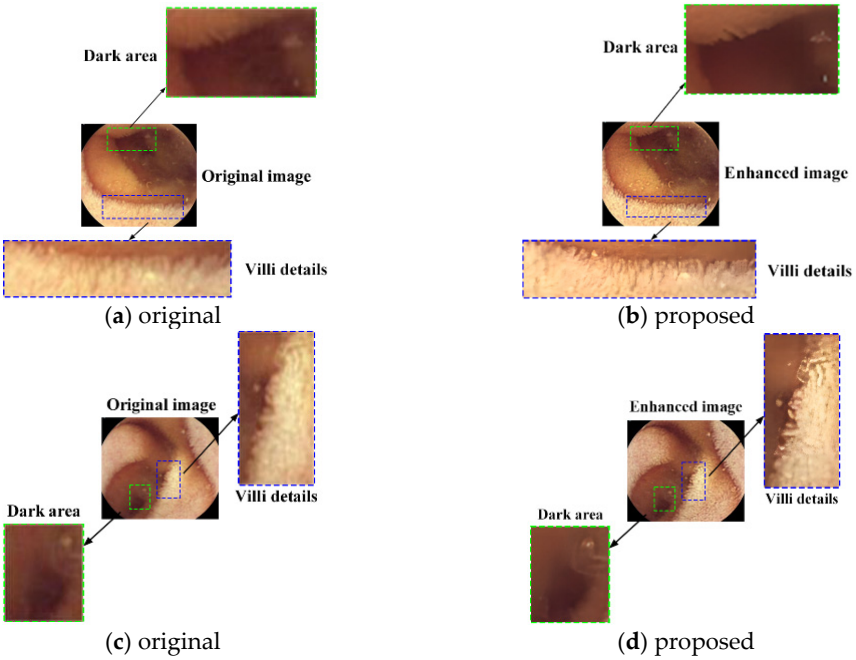

Figure 10. Selecting (**a**,**c**) from the original small intestine images in Figure 9e,g from the enhanced small intestine images in Figure 9, details were magnified. (**a**,**c**), respectively, correspond to Figure 9a,c, and (**b**,**d**), respectively, correspond to Figure 9e,g.

4.4. Experimental Comparison Analysis

In this paper, 50 WCE small intestine images were enhanced using HCUM [19], NLUM [20], UMGF [21], and the method of this paper. Table 2 shows the mean values of PSNR, IRMLE, and NIQE after processing by the above methods, where the best objective values are shown in bold. Figure 11a–c show the PSNR, IRMLE, and NIQE values for the

WCE small intestine images after each method individually processed them. In Table 2, although HCUM showed a decent IRMLE value, its PSNR and NIQE values were poor, indicating that using this method to enhance the details of WCE small intestine images may result in excessive noise enhancement. Additionally, the structure of the enhanced WCE small intestine images was altered. In Table 2, the IRMLE value of UMGF decreased compared to the original image. The WCE small intestine villus images enhanced using our method exhibited excessive brightness enhancement, resulting in detail enhancement occurring in excessively bright and excessively dark areas. Figure 12b,g,l show the results after HCUM enhancement, Figure 12d,i,n show the results after UMGF enhancement. We can observe that the WCE small intestine villi images enhanced by HCUM and UMGF exhibited excessive noise enhancement, structural changes, and edge overshooting. In Table 2, NLUM exhibited good PSNR, IRMLE, and NIQE values. Additionally, the NLUM enhancement results in Figure 12c,h,m reveal that the structure of the WCE small intestine villi image was well preserved without the occurrence of edge overshooting. However, there was an issue of excessive noise enhancement in the dark areas of the WCE small intestine image after enhancement.

Table 2. Average value of evaluation indicators using different methods.

Method	PSNR	IRMLE	NIQE
original	-	1.6640	4.7734
HCUM	19.8565	**2.4620**	5.2023
NLUM	31.3513	2.0271	**3.0818**
UMGF	19.7736	1.6555	3.9417
proposed	**34.4204**	1.8743	3.2532

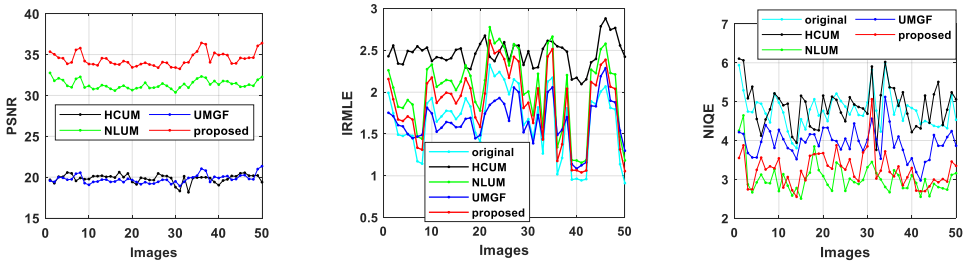

(**a**) PSNR (**b**) IRMLE (**c**) NIQE

Figure 11. Enhancement of 50 sets of small intestine images using different methods and evaluation of the enhancement results using assessment metrics.

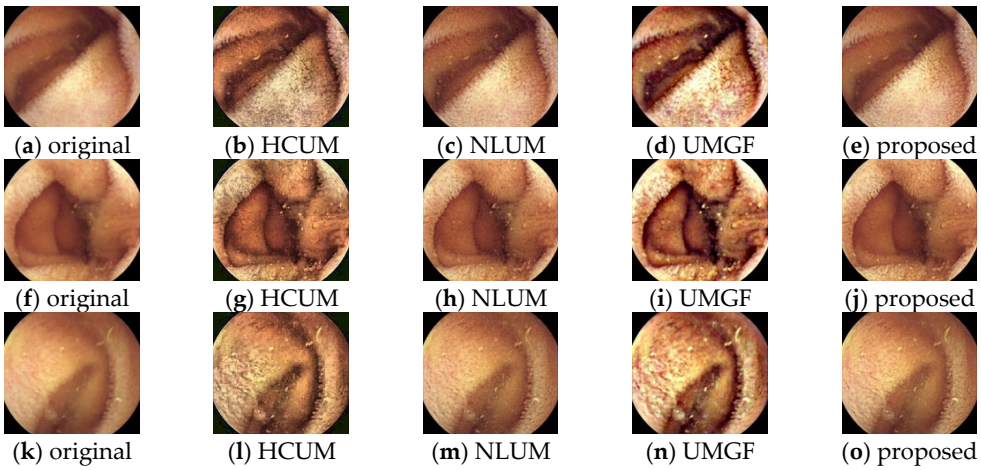

(**a**) original (**b**) HCUM (**c**) NLUM (**d**) UMGF (**e**) proposed

(**f**) original (**g**) HCUM (**h**) NLUM (**i**) UMGF (**j**) proposed

(**k**) original (**l**) HCUM (**m**) NLUM (**n**) UMGF (**o**) proposed

Figure 12. Three different sets of representative images of small intestine were selected and enhanced using HCUM, NLUM, UMGF, and the methods in this paper, respectively.

Compared to other methods, our approach yielded the highest average PSNR values for the enhanced WCE small intestine villus images, along with significant improvements in IRMLE and NIQE values. This suggests that our method effectively enhances the details of WCE small intestine villus images while suppressing the increase in noise, resulting in a visually pleasing enhancement. Moreover, as shown in Figure 12e,j,o depicting the results of this method, it also prevents the occurrence of edge artifacts.

To further verify the effectiveness of our method, the enhancement results of the above HCUM, NLUM, and UMGF methods were denoised using gaussian filters. Table 3 shows the mean values of PSNR, IRMLE, and NIQE after the denoising process, where the best objective values are shown in bold. Figure 13a–c show the denoised PSNR, IRMLE, and NIQE values of each WCE small bowel image. Figure 14 shows the results of HCUM, NLUM, and UMGF enhancement followed by denoising process.

Table 3. Average value of evaluation indicators using different methods after denoising.

Method	PSNR	IRMLE	NIQE
original	-	1.6640	4.7734
HCUM	21.0051	**2.3990**	3.9505
NLUM	31.9147	1.9353	4.5599
UMGF	20.0433	1.6610	5.1426
proposed	**34.4204**	1.8743	**3.2532**

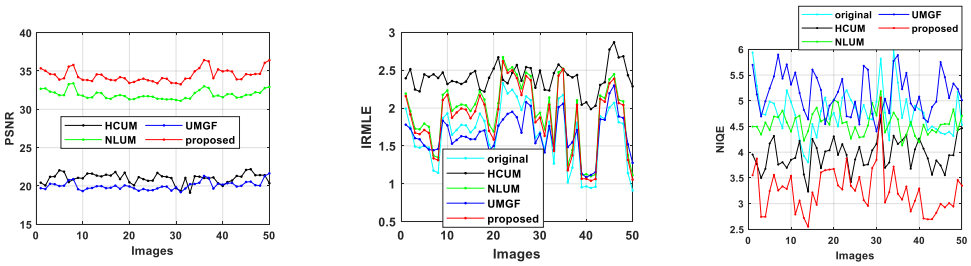

(**a**) PSNR (**b**) IRMLE (**c**) NIQE

Figure 13. Enhancement of 50 sets of denoised small intestine images using different methods and evaluation of the enhancement results.

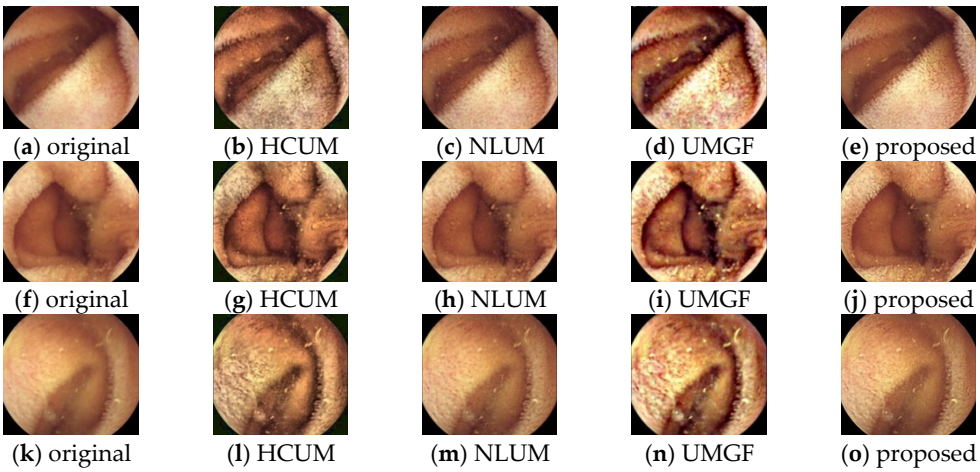

(**a**) original (**b**) HCUM (**c**) NLUM (**d**) UMGF (**e**) proposed

(**f**) original (**g**) HCUM (**h**) NLUM (**i**) UMGF (**j**) proposed

(**k**) original (**l**) HCUM (**m**) NLUM (**n**) UMGF (**o**) proposed

Figure 14. Three sets of representative small intestine image collections were selected and enhanced using HCUM, NLUM, UMGF, and our method, followed by denoising, respectively.

In Figure 14, after denoising, the enhancement results of HCUM, NLUM, and UMGF exhibited a noticeable reduction in noise. Compared to Table 2, the PSNR values in Table 3 have improved, and the IRMLE values have decreased. The mentioned alterations suggest

that WCE small intestine villi images enhanced through HCUM, NLUM, and UMGF contained excessive noise in the details, which affected both the enhancement of details and the preservation of the structure.

Moreover, compared to Table 2, in Table 3, the NIQE value of HCUM decreased after denoising, indicating an excessive amount of noise in the enhanced dark areas. The quality of the enhancement results improved after denoising. The NIQE values of NLUM and UMGF increased after denoising, indicating an excessive enhancement of details. Although there was a slight smoothing of details during noise removal, as seen in Figure 14, the problem of excessive enhancement still persisted. In Table 3, the PSNR and NIQE values after denoising with HCUM, NLUM, and UMGF still fell short of the method presented in this paper. This indicates that our method is capable of effectively emphasizing the details of small intestine villi while suppressing noise and preventing excessive enhancement. Furthermore, the clarity-enhanced small intestine villus images generated using our method exhibited good visual quality. It is crucial to highlight that our method's enhancement performance is not satisfactory for particularly dark areas, as evidenced by the experimental results in Figure 10. The main reason for this is the severe lack of information in those regions of the images.

In our study on enhancing small intestinal villi images, time efficiency is a critical consideration, particularly in scenarios like real-time endoscopic examinations. Our proposed method significantly improved processing speed while ensuring effective image enhancement. We conducted a detailed assessment of processing times for different methods, recording and analyzing their respective durations. Table 4 presents the average processing time per image and the total time for processing 50 small intestinal villi images for four methods: HCUM, NLUM, UMGF, and our proposed approach. The HCUM method had an average processing time of 0.087 s, resulting in a total time of 4.351 s. The NLUM method showed a relatively longer average time of 0.143 s, leading to a total of 7.185 s. The UMGF method had an average time of 0.088 s and a total processing time of 4.431 s.

Table 4. Processing time comparison of enhancement methods.

Method	Average Time	Total Time
HCUM	0.087 s	4.351 s
NLUM	0.143 s	7.185 s
UMGF	0.088 s	4.431 s
proposed	**0.014 s**	**0.712 s**

In contrast, our proposed method excelled in time efficiency, achieving an average processing time of only 0.014 s, with a total time of just 0.712 s. Notably, our approach does not require extensive training data or a complex training process; it leverages the analysis and processing of local image features to achieve rapid image enhancement. This makes it particularly suitable for real-time applications, ensuring the timeliness of images captured during capsule endoscopy. While HCUM, NLUM, and UMGF methods can achieve image enhancement to some extent, their lower time efficiency may result in insufficient effectiveness in real-time applications.

5. Discussion

1. Deficiencies of Existing Methods and Advantages of Our Method

At present, numerous enhancement methods for small intestine images have obvious defects when processing small intestine villus images. As for the method based on HE, it achieves image enhancement by remapping the probability distribution of gray levels. However, this approach fails to fully consider local features, resulting in unbalanced detail enhancement and amplification of noise. In contrast, the method adopted in this paper can process the information contained in different frequency regions more purposefully by separating the high-frequency and low-frequency components of the image. The Retinex-based

method is less effective when dealing with the microscopic small intestine villus structure and may cause halo effects and loss of naturalness. The light gain function and gradient gain function proposed by us focus on enhancing the details of small intestine villi. Specifically, by calculating the light gain factor from the low-frequency component and obtaining the gradient gain factor using the Laplacian convolution result, we can more accurately highlight the villus details and avoid the occurrence of the above problems. In addition, when the USM method enhances high-frequency components, due to the use of a fixed gain factor, it is very easy to cause edge overshoot and amplification of noise. In comparison, the method proposed in this paper has obvious advantages. The constructed adaptive gain factor can be dynamically adjusted according to light and gradient information, effectively preventing edge overshoot and suppressing noise while enhancing details. By constructing the light gain function and gradient gain function respectively to generate an adaptive gain factor, this method effectively overcomes a series of problems such as insufficient detail enhancement, noise amplification, and edge overshoot faced by traditional image enhancement methods in the process of small intestine villus image processing.

2. Experimental Results and Advantage Analysis

The experimental results based on 50 small intestine WCE images clearly show that this method has significant advantages over classic enhancement algorithms (HCUM, NLUM, UMGF). In terms of quantitative indicators, the PSNR of this method was increased by 45.47%, which fully reflects a significant improvement in image quality. The image was clearer and could provide more accurate visual information for doctors. The IRMLE was increased by 12.63% relative to the original image, further proving the excellent ability of this method in enhancing image details. Especially for the presentation of fine structures such as small intestine villi, it was more abundant and accurate, which could help doctors discover potential lesion features. The NIQE was reduced by 31.84%, meaning that this method is outstanding in noise suppression. It can effectively reduce the interference of noise on the image and better maintain the edge information of the image, making it perform better in aspects such as enhancement effect, noise suppression, and edge preservation. At the same time, this method also showed a high level of time efficiency, with an average processing time of only 0.014 s per image. This efficient processing speed shows its great potential in real-time applications and is very suitable for scenarios with high real-time requirements such as capsule endoscopy. In clinical practice, quickly obtaining clear and accurate images is crucial for timely diagnosis and treatment. Good objective data evaluation is a powerful proof of the performance of this method. At the same time, it clearly shows that it has significant superiority in clinical applications and can provide a more reliable basis for the diagnosis of small intestine diseases.

3. Clinical Significance and Application Value

From a clinical significance perspective, the morphology and details of small intestine villi are of crucial importance for accurate diagnosis of small intestine diseases. Our method significantly improves the clarity of the image, makes the villus edges more natural, and enriches the details. It helps doctors observe relevant details more clearly, thereby more accurately judging the lesion situation. For minor lesions, traditional methods often cannot effectively display the lesion location and characteristics, leading to an increased risk of misdiagnosis. Our method can better present minor lesions by enhancing villus details and suppressing noise, providing more accurate diagnostic information for doctors and significantly improving diagnostic accuracy. Our method provides more reliable diagnostic images for clinical use, reduces the possibility of misdiagnosis, and has the potential to obtain diagnostic images in real time while improving the overall accuracy of clinical diagnosis. This is of great significance for improving medical quality and treatment effects of patients.

4. Limitations of Our Method and Future Research Directions

Although our method significantly enhances the clarity of small intestinal villi, it still faces noise interference in darker regions of WCE images. This interference can weaken the algorithm's performance, resulting in image quality that falls short of ideal standards. Future work will focus on addressing this challenge by optimizing the enhancement method specifically for darker areas of the small intestine. We will investigate effective strategies to reduce noise interference and improve image detail presentation.

Additionally, we plan to conduct a pilot study in which doctors will review a series of original and enhanced images, providing feedback on diagnostic confidence and accuracy. We also aim to collaborate with medical institutions to develop a database of enhanced images and related clinical outcomes, facilitating further research and validation of our method's advantages.

6. Conclusions

This paper presents an image enhancement approach aimed at improving the clarity of small intestine villi. This approach aimed to address issues such as blurriness, detail loss, edge artifacts, and noise amplification in capsule endoscopy images capturing the villi-rich small intestine. By employing our method, doctors can observe and diagnose patients' conditions more accurately, providing stronger support for clinical diagnosis. Experimental results show that our proposed method achieved a 45.47% increase in PSNR compared to classical enhancement algorithms, a 12.63% improvement in IRMLE relative to the original images, and a 31.84% reduction in NIQE with respect to the original images.

Author Contributions: Conceptualization, S.Z. and Y.W. (Yinghui Wang); methodology, S.Z. and P.L.; software, Y.W. (Yukai Wang) and P.L.; validation, L.H.; data curation, M.W.; writing—original draft preparation, S.Z.; writing—review and editing, S.Z.; visualization, L.H.; supervision, M.W.; project administration, I.A. All authors have read and agreed to the published version of the manuscript.

Funding: This research was funded by the National Natural Science Foundation of China, grant number 62172190, the National Key Research and Development Program, grant number 2023YFC3805901, the "Double Creation" Plan of Jiangsu Province (Certificate: JSSCRC2021532), and partially by the "Taihu Talent-Innovative Leading Talent" Plan of Wuxi City (Certificate Date: 202110).

Data Availability Statement: The data used to support the findings of this paper are available from the corresponding authors upon request.

Conflicts of Interest: The authors declare no conflicts of interest.

References

1. Ghosh, T.; Fattah, S.A.; Wahid, K.A. CHOBS: Color histogram of block statistics for automatic bleeding detection in wireless capsule endoscopy video. *IEEE J. Transl. Eng. Health Med.* **2018**, *6*, 1–12. [CrossRef]
2. Widya, A.R.; Monno, Y.; Okutomi, M.; Suzuki, S.; Gotoda, T.; Miki, K. Stomach 3D reconstruction using virtual chromoendoscopic images. *IEEE J. Transl. Eng. Health Med.* **2021**, *9*, 1–11. [CrossRef] [PubMed]
3. Visible Body Suite (Version 4.31) [Computer Software]. 2023. Available online: www.visiblebody.com (accessed on 30 May 2023).
4. Kundu, A.K.; Fattah, S.A.; Wahid, K.A. Multiple linear discriminant models for extracting salient characteristic patterns in capsule endoscopy images for multi-disease detection. *IEEE J. Transl. Eng. Health Med.* **2020**, *8*, 1–11. [CrossRef]
5. Lien, G.S.; Liu, C.W.; Jiang, J.A.; Chuang, C.L.; Teng, M.T. Magnetic control system targeted for capsule endoscopic operations in the stomach—Design, fabrication, and in vitro and ex vivo evaluations. *IEEE Trans. Biomed. Eng.* **2012**, *59*, 2068–2079. [CrossRef]
6. Abdullah-Al-Wadud, M.; Kabir, M.H.; Dewan, M.A.A. A dynamic histogram equalization for image contrast enhancement. *IEEE Trans. Consum. Electron.* **2007**, *53*, 593–600. [CrossRef]
7. Wu, X.; Chen, H.; Gan, T. Automatic hookworm detection in wireless capsule endoscopy images. *IEEE Trans. Med. Imaging* **2016**, *35*, 1741–1752. [CrossRef]
8. Singh, N.; Bhandari, A.K. Principal component analysis-based low-light image enhancement using reflection model. *IEEE Trans. Instrum. Meas.* **2021**, *70*, 1–10. [CrossRef]
9. Thomas, G.; Flores-Tapia, D.; Pistorius, S. Histogram specification: A fast and flexible method to process digital images. *IEEE Trans. Instrum. Meas.* **2011**, *60*, 1565–1578. [CrossRef]
10. Brinkmann, B.H.; Manduca, A.; Robb, R.A. Optimized homomorp-hic unsharp masking for MR grayscale inhomogeneity correction. *IEEE Trans. Med. Imaging* **1998**, *17*, 161–171. [CrossRef]

11. Wang, N.N.; Wang, B.; Wang, W.P.; Guo, X.H. Computing medial axis transform with feature preservation via restricted power diagram. *ACM Trans. Graph.* **2012**, *20*, 209–212. [CrossRef]
12. Morel, J.M.; Petro, A.B.; Sbert, C. A PDE formalization of Retinex theory. *IEEE Trans. Image Process.* **2010**, *19*, 2825–2837. [CrossRef] [PubMed]
13. Zhang, H.; Wang, Y.; Ning, X.; Lv, K.; Wang, N. Volume Data Denoising via Extended Weighted Least Squares. *IEEE Access* **2019**, *7*, 2750–2758. [CrossRef]
14. Zhou, M.; Jin, K.; Wang, S.; Ye, J.; Qian, D. Color retinal image enhancement based on luminosity and contrast adjustment. *IEEE Trans. Biomed. Eng.* **2018**, *65*, 521–527. [CrossRef]
15. Xu, J.; Hou, Y.; Ren, D. Star: A structure and texture aware Retinex-model. *IEEE Trans. Image Process.* **2020**, *29*, 5022–5037. [CrossRef] [PubMed]
16. Kansal, S.; Purwar, S.; Tripathi, R.K. Trade-off between mean brightness and contrast in histogram equalization technique for image enhancement. In Proceedings of the 2017 IEEE International Conference on Signal and Image Processing Applications (ICSIPA), Kuching, Malaysia, 12–14 September 2017; pp. 195–198.
17. Land, E.H. The Retinex theory of color vision. *Sci. Am.* **1977**, *237*, 108–129. [CrossRef] [PubMed]
18. Xiao, C.; Shi, Z. Adaptive bilateral filtering and its application in Retinex image enhancement. In Proceedings of the 2013 Seventh International Conference on Image and Graphics, Qingdao, China, 26–28 July 2013; pp. 45–49.
19. Long, M.; Xie, X.; Li, G. Wireless capsule endoscopic image enhancement method based on histogram correction and unsharp masking in wavelet domain. In Proceedings of the 2019 17th IEEE International New Circuits and Systems Conference (NEWCAS), Munich, Germany, 23–26 June 2019; pp. 1–4.
20. Ngo, D.; Lee, S.; Kang, B. Nonlinear unsharp masking algorithm. In Proceedings of the 2020 International Conference on Electronics, Information, and Communication (ICEIC), Barcelona, Spain, 19–22 January 2020; pp. 1–6.
21. Shi, Z.; Chen, Y.; Gavves, E. Unsharp mask guided filtering. *IEEE Trans. Image Process.* **2021**, *30*, 7472–7485. [CrossRef]
22. Imtiaz, M.S.; Mohammed, S.K.; Deeba, F. Tri-Scan: A three stage color enhancement tool for endoscopic images. *J. Med. Syst.* **2017**, *41*, 1–16. [CrossRef]
23. Fang, S.; Xu, C.; Feng, B. Spatial entropy quartiles-based texture-aware fractional-order unsharp masking for visibility enhancement of remotely sensed images. *IEEE Trans. Syst. Man Cybern.* **2022**, *52*, 2275–2288.
24. Polesel, A.; Ramponi, G.; Mathews, V.J. Image enhancement via adaptive unsharp masking. *IEEE Trans. Image Process.* **2000**, *5*, 505–510. [CrossRef]
25. Wang, T.; Hong, S.; Liu, Y. Unsharp masking algorithm based on top-hat transform. *Comput. Eng. Des.* **2014**, *35*, 198–202.
26. Liu, P.X.; Wang, Y.H.; Yang, J.L.; Li, W. An adaptive enhancement method for gastrointestinal low-light images of capsule endoscope. In Proceedings of the ICASSP 2023—2023 IEEE International Conference on Acoustics, Speech and Signal Processing (ICASSP), Rhodes Island, Greece, 4–10 June 2023; pp. 1–5.
27. Kim, G.J.; Lee, S.; Kang, B. Single image haze removal using hazy particle maps. *IEICE Trans. Fundam. Electron. Commun. Comput. Sci.* **2018**, *101*, 1999–2002. [CrossRef]
28. He, K.; Sun, J.; Tang, X. Guided image filtering. *IEEE Trans. Pattern Anal. Mach. Intell.* **2012**, *35*, 1397–1409. [CrossRef]
29. Li, Z.; Zheng, J.; Zhu, Z. Weighted guided image filtering. *IEEE Trans. Image Process.* **2014**, *24*, 120–129. [PubMed]
30. Mittal, A.; Soundararajan, R.; Bovik, A.C. Making a completely blind image quality analyzer. *IEEE Signal Process. Lett.* **2012**, *20*, 209–212. [CrossRef]